Functional & Integrative Genomics (2023) 23:335
https://doi.org/10.1007/s10142-023-01260-4

ORIGINAL ARTICLE

# Long noncoding RNA LINC00482 silencing sensitizes non-small cell lung cancer cells to cisplatin by downregulating CLASRP via E2F1

Yanming Lin[1] · Jinmei Li[1] · Shujun Li[1] · Yuting Chen[1] · Yiping Luo[1] · Yongcun Wang[1] · Zhixiong Yang[1]

Received: 7 July 2023 / Revised: 9 October 2023 / Accepted: 20 October 2023 / Published online: 15 November 2023


## Abstract

Long noncoding RNA LINC00482 (LINC00482) is dysregulated in non-small cell lung cancer cells (NSCLC). Herein, this research examined the actions and specific mechanisms of LINC00482 in cisplatin (DDP) resistance in NSCLC. LINC00482 expression was assessed using RT-qPCR in clinical NSCLC tissues and cell lines. Knockdown and ectopic expression assays were conducted in A549 and HCC44 cells, followed by determination of cell proliferation with CCK-8 and clone formation assays, apoptosis with flow cytometry, and DDP sensitivity. The association between LINC00482, E2F1, and CLASRP was evaluated with dual-luciferase reporter, ChIP, and RIP assays. The role of LINC00482 in NSCLC was confirmed in nude mice. NSCLC tissues and cells had upregulated LINC00482 expression. LINC00482 was mainly localized in the cell nucleus, and LINC00482 recruited E2F1 to enhance CLASRP expression in NSCLC cells. LINC00482 knockdown enhanced the DDP sensitivity and apoptosis of NSCLC cells while reducing cell proliferation, which was negated by overexpressing CLASRP. LINC00482 knockdown restricted tumor growth and enhanced DDP sensitivity in NSCLC in vivo. LINC00482 silencing downregulated CLASRP through E2F1 to facilitate the sensitivity to DDP in NSCLC.

**Keywords** Long noncoding RNA LINC00482 · E2F transcription factor 1 · CLASRP · Non-small cell lung cancer · Cisplatin resistance

## Introduction

Lung cancer is a primary reason for cancer mortality because of its early metastasis, rapid growth, and highly malignant nature (Fan and Wu 2022). Non-small cell lung cancer (NSCLC) constitutes around 80–85% of lung cancers and includes two primary subtypes: lung squamous carcinoma (LUSC) and adenocarcinoma (LUAD) (Suster and Mino-Kenudson 2020; Zhang et al. 2022a, b). In general, NSCLC management depends on its stage (Dohopolski et al. 2021). Cisplatin (DDP)-based compounds are applied for adjuvant chemotherapy and the treatment of advanced NSCLC (Kryczka et al. 2021). Despite apparent improvements in clinical outcomes for NSCLC patients, NSCLC is still an incurable illness for the majority of patients and its therapy remains confronted with two main barriers: metastasis and chemotherapy resistance (Miller and Hanna 2021; Xie et al. 2022). Therefore, the discovery of mechanisms affecting DDP sensitivity can be beneficial for NSCLC management.

Dysregulated transcription of long non-coding RNAs (lncRNAs) holds pivotal functions in drug resistance, metastasis, and proliferation of lung cancer (Sun et al. 2019). Of note, LINC00482 exhibit high expression in LUSC cell lines (Zhang et al. 2022a, b), suggesting that LINC00482 may assume a role in NSCLC progression. Moreover, LncMAP website analyses in our study predicted that LINC00482 might regulate CLASRP expression by orchestrating E2F transcription factor 1 (E2F1) to influence NSCLC progression. E2F1 is a typical and well-studied member of the E2F family which modulates S-phase cyclin and gene transcription needed for DNA repair, apoptosis, and DNA replication (Fouad et al. 2020). Mounting evidence implicates the involvement of E2F1 in chemoresistance, cell proliferation, clone formation, stemness, apoptosis, and migration in cancers (Lin et al. 2021; Lu et al. 2018).

✉ Yongcun Wang
wycdiyi@163.com

✉ Zhixiong Yang
yangzhixiong068@126.com

[1] Department of Pulmonary Oncology, Affiliated Hospital of Guangdong Medical University, Zhanjiang, Guangdong 524000, People's Republic of China

Moreover, a prior study unveiled that E2F1 activation led to DDP resistance in liver carcinoma (Wang et al. 2021). E2F1 modulates the lncRNA MCF2L antisense RNA 1/embryonic lethal vision-like protein 1/Cyclin D1 axis to enhance NSCLC cell resistance to gefitinib (Shan et al. 2022). In addition, CLASRP, a protein-encoding gene, can act as an alternative splicing regulator and modulate CLK kinases (Xu et al. 2019). CLASRP was reported as an independent prognostic factor for patients with head and neck cancer (Liang et al. 2019). Nevertheless, little is known regarding the function of CLASRP in NSCLC.

Thus, we hypothesized that LINC00482 might modulate DDP resistance in NSCLC through the E2F1/CLASRP axis. Herein, this research examined the actions and specific mechanisms of LINC00482 in resistance to DDP in NSCLC via the E2F1/CLASRP axis.

## Materials and methods

### Ethics statement

Patients and their families were informed about this study and signed the informed consent forms. The experiments involving clinical samples were ratified by the medical ethics committee of Affiliated Hospital of Guangdong Medical University and conformed to the *Declaration of Helsinki*. All operations involving animals complied with the international ethical conventions for laboratory animals and the relevant national regulations.

### Clinical specimen collection

This study enrolled 90 patients (age: 43–75 years; the mean age: 56.21 ± 5.52 years) with NSCLC who received surgery in Affiliated Hospital of Guangdong Medical University between October 2021 and October 2022, of whom 59 were male and 31 were female. There were 52 cases of adenocarcinoma, 35 cases of squamous carcinoma, and 3 cases of adenosquamous carcinoma. All patients met the diagnostic criteria for NSCLC, were diagnosed by clinicopathological histology, and were in the tumor-node-metastasis (TNM) stage I-III. Additionally, none of patients were comorbid with other malignant tumors (such as gastric cancer and liver cancer) and serious chronic diseases (including hypertension, diabetes, and autoimmune diseases), had undergone anti-tumor treatments, developed serious cardiac, hepatic, or renal insufficiency and distant metastasis of tumors, and had a history of mental diseases or inability to communicate normally. Tissues from surgically removed cancerous and benign lesions were collected.

### Cell culture and lentivirus transfection

NSCLC cell lines A549 and HCC44 and human normal lung epithelial BEAS-2B cells (iCell Bioscience, Shanghai, China) were cultivated with 1640 medium encompassing 100 U/mL of penicillin/streptomycin and 10% fetal bovine serum in an incubator (37 °C, 5% $CO_2$).

Short hairpin RNA (shRNA) vectors were introduced in A549 and HCC44 cells by lentiviral infection. For lentivirus preparation, shRNA vectors, psPAX2 (BR036, FengHuiShengWu, Changsha, China), and pMD2.G (BR037, FengHuiShengWu) at a ratio of 4:3:2 were transfected in HEK293T cells using Lipofectamine 3000 (L3000015, Thermo Fisher Scientific, Wilmington, DE, USA). Briefly, 10 μg shRNA plasmids, 7.5 μg psPAX2, and 5 μg pMD2.G were transfected in HEK293T cells in a 100 mm culture dish. After transfection for 48 h, cells were subjected to centrifugation at 1000 g for 30 min. The virus supernatant was attained after filtration (0.45 μm) and transduced into cells using 8 μg/mL polyamine. Following 48-h transduction, cells were screened with puromycin and validated by real-time polymerase chain reaction (PCR) (Wang et al. 2022).

### Cell transfection

Depending on transfection, cells were assigned into control, negative control (NC) shRNA, LINC00482 shRNA#1, LINC00482 shRNA#2, LINC00482 shRNA#3, overexpression (oe)–NC, oe-LINC00482, oe-NC + NC shRNA, oe-LINC00482 + NC shRNA, oe-LINC00482 + E2F1 shRNA, LINC00482 shRNA + oe-CLASRP, LINC00482 shRNA + oe-NC, and LINC00482 shRNA + oe-CLASRP groups. All target plasmids were bought from WZ Biosciences (Shandong, China). Cell density was adjusted based on cell growth rate, and cells were spread in 6-well plates to allow cells reaching 70–80% confluence on the second day and transfected using Lipofectamine 3000. Target plasmids (4 μg) and Lipofectamine 3000 (10 μL) were respectively diluted with Opti-minimal essential medium (MEM) (250 μL; Gibco, Grand Island, NY, USA), left to stand at ambient temperature for 5 min, and then mixed. Following 20-min standing, the mixed solution was supplemented to the wells transfection. After 8 h, the medium was refreshed. As a control, the cells in the control group were treated with PBS. After 12–16 h of cell recovery, cells were treated with corresponding concentrations of DDP for 48 h and collected (Tan et al. 2022). The LINC00482 shRNA sequences were shown below: LINC00482 shRNA#1: CCCAATAAGGTC CCATTCTGA; LINC00482 shRNA#2: CAAGGACATTCC TGTGGTTCT; and LINC00482 shRNA#3: CTAAGTATA GTCAGCAGTGAT.

## Reverse transcription-quantitative PCR (RT-qPCR)

A reverse transcription kit (RR047A, Takara, Shiga, Japan) was applied to reverse transcribe the total RNA, which was extracted from cells or tissue samples using TRIzol (15596026, Invitrogen, San Diego, CA, USA), into cDNA. The system was 20 μL and the reaction conditions were 15 min at 37 °C and 5 s at 85 °C. Samples (three replicates per sample) were loaded using 2 × SYBR Green PCR Mastermix (SR1110, Solarbio, Beijing, China) and subjected to RT-qPCR reactions in a real-time fluorescence quantitative PCR instrument (ABI7500, Applied Biosystems, Foster City, CA, USA). The reaction system contains SYBR Mix (9 μL), positive primers (0.5 μL), negative primers (0.5 μL), cDNA (2 μL), and RNase Free dH2O (8 μL). The reaction conditions were set to 95 °C for 10 min, 95 °C for 15 s, and 60 °C for 1 min for 40 consecutive cycles. Primers (Table 1) were synthesized by Sangon (Shanghai, China). Cycle threshold (Ct) values of wells were recorded, and product relative expression was calculated using the $2^{-\Delta\Delta Ct}$ method with glyceraldehyde-3-phosphate dehydrogenase (GAPDH) as a normalizer (Ayuk et al. 2016).

Intracellular and nuclear RNAs were extracted. Specifically, cells received twice washes with pre-chilled phosphate-buffered saline (PBS), and the cell precipitates were gently resuspended in hypotonic solution, treated for 10 s with NP40, and centrifuged for 10 min at 3000 rpm and 4 °C. The supernatants, which are the cytoplasmic contents, were added with equivalent volume of chloroform and centrifuged for 10 min at 4 °C. The supernatants were transferred to new clean tubes and mixed with equivalent volume of ethanol, and the intracellular RNAs were extracted per the instructions. The intracellular precipitates were resuspended, rinsed once with pre-chilled PBS, and centrifuged for 10 min at 4 °C to discard the supernatants. Afterward, TRIzol (1 mL) was added for nuclear RNA extraction. U6 small nuclear RNA and GAPDH served as the normalizers for nuclear and cytoplasmic RNAs, respectively (Zhang et al. 2018).

**Table 1** Primers for RT-qPCR

| Names | Sequences |
|---|---|
| LINC00482 | F: 5'-AGGGGTAACCTACCGGGAAA-3' |
| | R: 5'-CTTGGCCAGAGCTCCAGAAG-3' |
| E2F1 | F: 5'-CCGTGGACTCTTCGGAGAAC-3' |
| | R: 5'-ATCCCACCTACGGTCTCCTC-3' |
| CLASRP | F: 5'-GAAGAAGGCATCCATCGGCTACAC-3' |
| | R: 5'-GCATCCTGACGAAGTCGCCATC-3' |
| GAPDH | F: 5'-CCATGTTCGTCATGGGTGTGAACCA-3' |
| | R: 5'-GCCAGTAGAGGCAGGGATGATGTTC-3' |
| U6 | F: 5'-AAAGCAAATCATCGGACGACC-3' |
| | R: 5'-GTACAACACATTGTTTCCTCGGA-3' |

## Western blotting

On ice, cells and prepared tissue homogenates were lysed with Radio-Immunoprecipitation assay (RIPA) protein lysis solution (P0013B, Beyotime, Shanghai, China) for 10 min. Bicinchoninic acid quantification kits (P0012S, Beyotime) was applied for protein quantifications. Proteins were boiled for 10 min with 10 μL loading buffer at 95 °C and subjected to sodium dodecyl sulfate polyacrylamide gel electrophoresis at the 100 V lane. Then, proteins were transferred to nitrocellulose membranes with 30 mA current for 120 min, and the membranes were sealed with 5% bovine serum albumin/Tris-buffered saline with Tween 20 (TBST) at ambient temperature for 60 min. Subsequently, the membranes were probed with primary antibodies of anti-E2F1 (#3742, 1:100, Cell Signaling Technology [CST], Beverly, MA, USA), anti-CLASRP (sc-514890, 1:500, Santa Cruz Biotechnology, Dallas, TX, USA), anti-GAPDH (#5174, 1:5000, CST) overnight at 4 °C. The membranes received 1 × TBST solution washes (3 times × 5 min) on a shaker at ambient temperature, 2-h hybridization with horseradish peroxidase-labeled secondary antibodies of goat anti-rabbit immunoglobulin G (IgG) H&L (ab6721, 1:5000, Abcam, Cambridge, UK) and goat anti-mouse IgG (ab6789, 1:5000, Abcam) at ambient temperature, and TBST washes (3 times × 20 min). The luminescence reaction was conducted with an enhanced chemiluminescence kit. Then, protein blots were observed, followed by image analyses. Band grayscale values were analyzed with Image J software, and the relative expression of target proteins was denoted as the grayscale value of target bands/the grayscale value of internal reference.

## Cell counting kit (CCK)-8 assay

Following digestion and resuspension, transfected cells were adjusted to $1 \times 10^5$ cells/mL and seeded and cultivated overnight in 96-well plates (100 μL/well). The cells were treated as per the directions of CCK-8 kits (C0037, Beyotime), and their cell viability was assessed by CCK-8 method at the 24th, 48th, 72nd, and 96th h after seeding, respectively. For each assessment, the cells were supplemented with 10 μL CCK-8 assay solution and incubated for 4 h in an incubator. The absorbance at 450 nm was examined using a microplate reader, followed by plotting of growth curves.

## Clone formation assay

Logarithmically growing cells were prepared into single-cell suspensions, counted, seeded in culture dishes (1,000 cells per 60 mm dish), and cultured in a $CO_2$ incubator.

The medium was renewed every 3 d. Following 14 d of culture, the medium was discarded, and cells received 15-min methanol fixation and 15-min crystal violet staining. Then, the colonies of more than 50 cells were counted under a microscope.

## Flow cytometry

Apoptosis of DDP-stimulated cells was assessed using Annexin V/propidium iodide (PI) apoptosis assay kits (CA1020, Solarbio). Cells were blown apart after digestion using ethylene diamine tetraacetic acid-free trypsin and collected into centrifuge tubes for centrifugation. The supernatants were discarded, and cells received twice PBS washes, drying, and resuspension in 1 × binding buffer. Cell suspension (100 μL) was transferred to a flow tube (5 mL), mixed and incubated for 5 min with Annexin V/fluorescein isothiocyanate (FITC) (5 μL) at ambient temperature in dark, and supplemented with PI solution (5 μL) and PBS (400 μL). After reaction termination, apoptosis rates were determined immediately using FACSCanto II flow cytometer (BD Bioscience, Franklin Lakes, New Jersey, USA).

## Dual-luciferase reporter assay

NC shRNA and LNC00482 shRNA were co-transfected with CLASRP-2 Kb luciferase reporter plasmids into A549 cells to test the influence of LINC00482 on the CLASRP promoter activity, respectively. Forty-eight h after transfection, cells were lysed, and the assay was conducted using a luciferase reporter gene assay kit (RG005, Beyotime) with a dual-luciferase reporter gene assay system (Promega, Madison, WI, USA). The activation degree of target reporter genes was assessed by the ratio of relative light unit between Firefly/Renilla (internal reference) luciferases.

The presence of binding sites of E2F1 protein to CLASRP DNA was predicted via the JASPAR website. Recombinant luciferase reporter gene vectors with mutated binding sites were constructed and co-transfected with oe-E2F1/oe-NC into A549 cells, followed by dual-luciferase reporter assays to verify the specific binding sites of E2F1 protein to CLASRP DNA. The specific steps were the same as above.

## Chromatin immunoprecipitation (ChIP) assay

A549 cells received 10-min formaldehyde fixation to produce DNA–protein crosslinks and were fragmented through 15 cycles of 10-s sonication at an interval of 10 s, and 10-min centrifugation at 12,000 g and 4 °C. The supernatants were separated into two tubes (10 μg chromatin per immunoprecipitation) and incubated overnight with normal mouse IgG antibodies (5 μg, ab172730, 1:100, Abcam) and rabbit E2F1 antibodies (5 μg, #3742, 1:100, CST), respectively, at 4 °C for full binding. DNA–protein complexes were precipitated with Protein Agarose/Sepharose and centrifuged for 5 min at 12,000 g, and the supernatants were discarded. The non-specific complexes received washes and overnight de-crosslinking at 65 °C, followed by DNA fragment extraction, purification, and recovery with phenol/chloroform for RT-qPCR.

After LINC00482 silencing, samples containing purified DNA fragments were finally attained for ChIP assays (same steps as above) to examine changes in E2F1 enrichment at the CLASRP promoter, followed by RT-qPCR.

## RNA immunoprecipitation (RIP) assay

The binding of LINC00482 to E2F1 was assessed using RIP kits (Millipore, Billerica, MA, USA). Cells received lysing (5 min in an ice bath) with an equal volume of RIPA lysis solution (P0013B, Beyotime) and centrifugation (10 min, 14,000 g, 4 °C), after which the supernatants were removed. Cell extracts and antibodies were co-precipitated via incubation: magnetic beads (50 μL) received washes and resuspension in RIP wash buffer (100 μL) and incubation with antibodies (1 μg) for binding. Magnetic bead-antibody complexes received washes and resuspension in RIP wash buffer (900 μL) before overnight incubation with cell extracts (100 μL) at 4 °C. The sample was placed on a magnetic holder to collect magnetic bead-protein complexes which were digested using proteinase K to retrieve RNA for PCR. The antibodies used for RIP included E2F1 antibodies (#3742, 1:100, CST) which were mixed with the sample at room temperature for 30 min and IgG antibodies (ab172730, 1:100, Abcam).

## Fluorescence in situ hybridization (FISH)

The subcellular localization of LINC00482 in NSCLC cell lines was identified using the FISH Kit for RNA (R0306S, Beyotime). Briefly, NSCLC cells were seeded in 6-well plates. When cell confluence reached about 80%, cells received fixation, permeabilization, and pre-hybridization before cells were immersed in hybridization solution containing probes, sealed, and placed in a shaker at 45–65 °C in dark for overnight hybridization. Subsequent to 4',6-Diamidino-2-Phenylindole staining, cells were sealed with anti-fluorescent bursting agent, observed under a fluorescent microscope (Olympus, Tokyo, Japan), and imaged.

## Tumor-bearing mouse assay

BALB/c nude mice (weighing 16 ± 2 g, aged 4–5 weeks, Vital River Laboratories, Beijing, China) were reared in an environment with constant temperature (25–27 °C) and humidity (45%-50%). Nude mice were randomly allocated

into four groups (NC shRNA + dimethyl sulfoxide [DMSO], NC shRNA + DDP, LINC00482 shRNA + DMSO, and LINC00482 shRNA + DDP; six mice/group) (Wang et al. 2022). Briefly, nude mice were subcutaneously injected with 50 µL stably transfected A549 cell suspension ($1 \times 10^7$ cells/mL) into the back and injected with 4 mg/kg DDP or DMSO via tail vein after 7 days (Tan et al. 2022). The tumor growth was closely observed. The longest (a) and shortest (b) diameters of tumors were measured every 7 days, and tumor volumes were calculated to plot the growth curve with the formula: $(a \times b^2)/2$ (Kun-Peng et al. 2017). Nude mice were euthanized after 28 days. The tumors were peeled off, weighed, and photographed, and tumor tissues were harvested for assays.

### Immunohistochemical staining

Tumor tissues received 4% paraformaldehyde fixation, paraffin embedding, and sectioning, and the sections were subjected to immunohistochemical staining (Tan et al. 2022). Following xylene dewaxing and ethanol dehydration at different concentrations, sections were antigenically repaired with 0.01 M sodium citrate solution, incubated for 10 min with 3% $H_2O_2$, and sealed for 30 min with goat serum at room temperature. Sections underwent incubation with anti-Ki67 antibodies (ab15580, 1:1000, Abcam) (overnight, 4 °C) and with goat anti-rabbit IgG H&L (ab6721, 1:1000, Abcam) (1 h, room temperature), followed by diaminobenzidine and hematoxylin staining and neutral gum sealing. Observations and photographs were conducted using a microscope (Olympus), and positive expression was analyzed using Image J.

### Statistical analyses

All data were statistically analyzed using Graphpad 8.0. The measurement data were displayed in the form of mean ± standard error of mean. Comparisons between two groups were analyzed via the paired or unpaired *t*-test, and comparisons among multiple groups were analyzed using one-way analysis of variance with Tukey's tests for post hoc multiple comparisons. $P < 0.05$ illustrated that the difference was statistically significant.

## Results

### LINC00482 expression was high in NSCLC tissues and cells

With reference to previous work (Zhang et al. 2022a, b)), the analyses of the lncRNA microarray in the Gene Expression Omnibus database identified 11 differentially expressed lncRNAs in lung cancer (LINC00482, C10orf55, AC130462.2, AC104785.1, AP005899.1, AC138035.1, AL021154.1, AC10422.4, MIR3945HG, AC008734.1, and LINC02408), of which LINC00482 was used as the study target. RT-qPCR data exhibited that LINC00482 expression was dramatically higher in 90 NSCLC tissues versus that in adjacent tissues (Fig. 1A, $P < 0.05$). In addition, LINC00482 expression was not correlated with gender, age, and pathological type but was correlated with tumor diameter, TNM staging, and lymph node metastasis in patients with NSCLC (Table 2, $P < 0.05$). Specifically, patients with tumor diameter ≥ 3 cm, stage III NSCLC, and lymph node metastasis had higher LINC00482 expression. RT-qPCR also displayed that both A549 and HCC44 cells had apparently higher LINC00482 expression than BEAS2B cells (Fig. 1B, $P < 0.05$). In conclusion, LINC00482 was overexpressed in NSCLC tissues and cells.

### LINC00482 inhibited NSCLC cell sensitivity to DDP

To clarify the influence of LINC00482 on NSCLC cell sensitivity to DDP, A549 and HCC44 cells were infected with LINC00482 shRNA lentiviruses and treated with different concentrations of DDP (the cells treated with PBS were named as the control group). RT-qPCR results manifested that LINC00482 shRNA#1, #2, and #3 markedly lowered LINC00482 expression in cells (Fig. 2A, $P < 0.05$). CCK-8 assay data displayed that LINC00482 shRNA#1, #2, and #3 conspicuously reduced A549 and HCC44 cell viability, with the most evident decrease upon LINC00482 shRNA#3. The half-inhibitory concentration (IC50) of DDP for A549 and HCC44 cells was 6.87 and 7.38 µg/mL, respectively (Fig. 2B-D, $P < 0.05$). Clone formation assay and flow cytometry data documented that LINC00482 shRNA#1, #2, and #3 appreciably reduced clonogenicity and elevated apoptosis of A549 cells (Fig. 2E-H, $P < 0.05$). The above experimental results also revealed that the variable transfection efficiency of different LINC00482 shRNAs in different cells resulted in the differences in gene and protein expression levels, ultimately affecting the biological functions of cells. LINC00482 shRNA#3 showed the most significant changes. Therefore, subsequent cell rescue experiments and in vitro and in vivo assays were conducted upon the transfection with LINC00482 shRNA#3, which was uniformly expressed as LINC00482 shRNA below.

To further verify the effects of LINC00482 on NSCLC cell sensitivity to DDP, NSCLC cells were transfected with oe-LINC00482, followed by transfection efficiency determination using RT-qPCR. As reflected in Supplementary Fig. 1A ($P < 0.05$), the oe-LINC00482 group had obviously increased expression of LINC00482 compared with the oe-NC group. CCK-8 assay revealed that oe-LINC00482 transfection significantly improved the

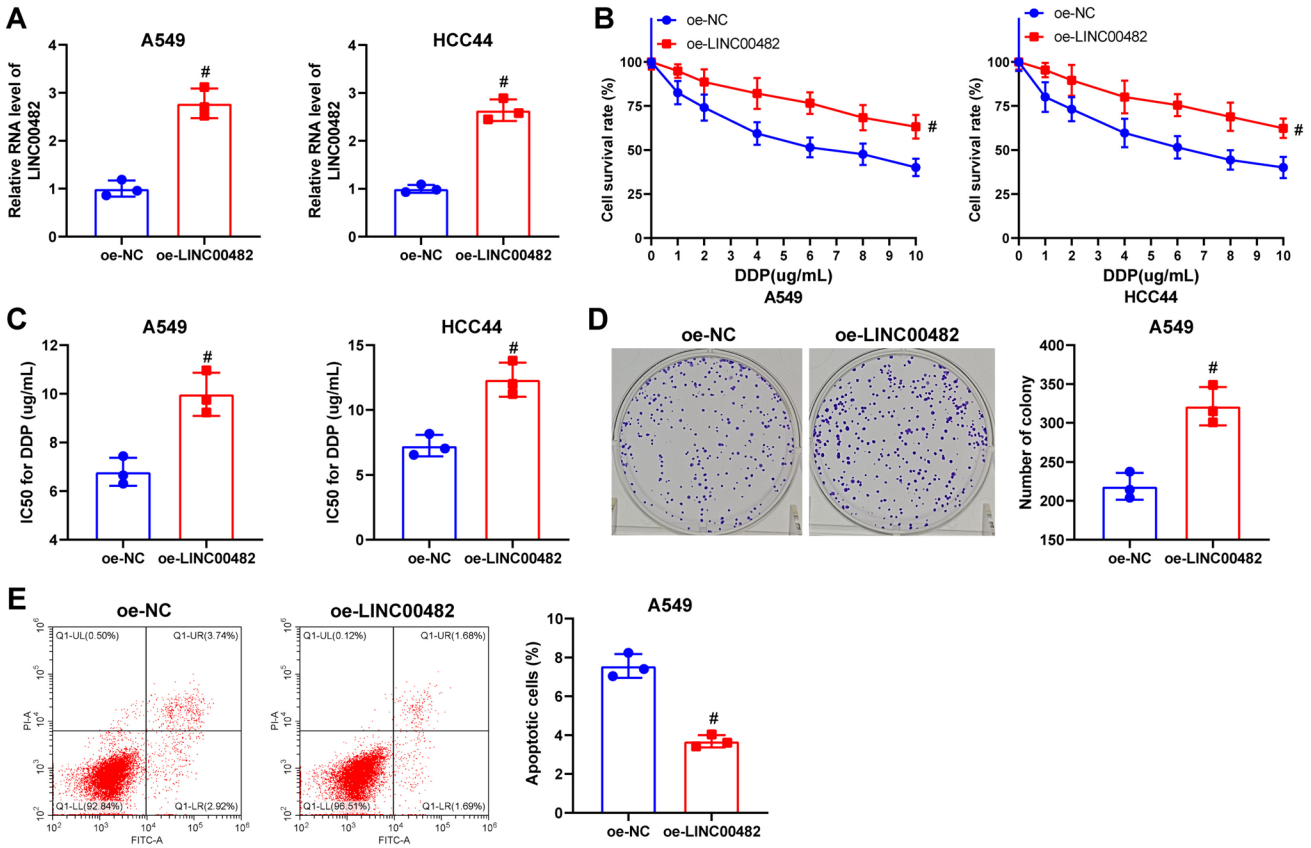


**Fig. 1** NSCLC tissues and cells have upregulated LINC00482 expression. Note: **A**: RT-qPCR detection of LINC00482 expression in human NSCLC and adjacent tissues ($n=90$). **B**: RT-qPCR detection of LINC00482 expression in human NSCLC cell lines A549 and HCC44 ($n=3$). The measurement data were displayed as mean ± standard error of mean. Comparisons among multiple groups were performed using one-way analysis of variance. * indicates $P<0.05$ compared with adjacent tissues; # indicates $P<0.05$ compared with BEAS2B cells. NSCLC, non-small cell lung cancer

**Table 2** Relationship between LINC00482 expression and clinical profiles of patients with non-small cell lung cancer

| Clinical characteristics | | Case number | Mean ± standard error of mean | *P* value |
|---|---|---|---|---|
| Gender | Male | 59 | 3.48 ± 1.53 | 0.562 |
| | Female | 31 | 3.22 ± 2.45 | |
| Age | < 60 years old | 56 | 3.12 ± 2.11 | 0.232 |
| | ≥ 60 years old | 34 | 3.58 ± 1.52 | |
| Pathological type | Adenocarcinoma | 52 | 3.26 ± 2.13 | 0.677 |
| | Squamous carcinoma | 35 | 3.39 ± 2.44 | |
| | Adenosquamous carcinoma | 3 | 3.56 ± 2.82 | |
| Tumor diameter (cm) | < 3 | 49 | 3.01 ± 1.82 | 0.0288* |
| | ≥ 3 | 41 | 3.74 ± 1.15 | |
| Tumor-node-metastasis (TNM) stage | Stage I | 22 | 2.93 ± 0.74 | 0.002* |
| | Stage II | 53 | 3.34 ± 1.18 | |
| | Stage III | 15 | 3.86 ± 1.25 | |
| Lymph node metastasis | Yes | 29 | 3.98 ± 2.34 | 0.0466* |
| | No | 61 | 3.02 ± 1.32 | |

* indicates $P<0.05$, the difference was statistically significant

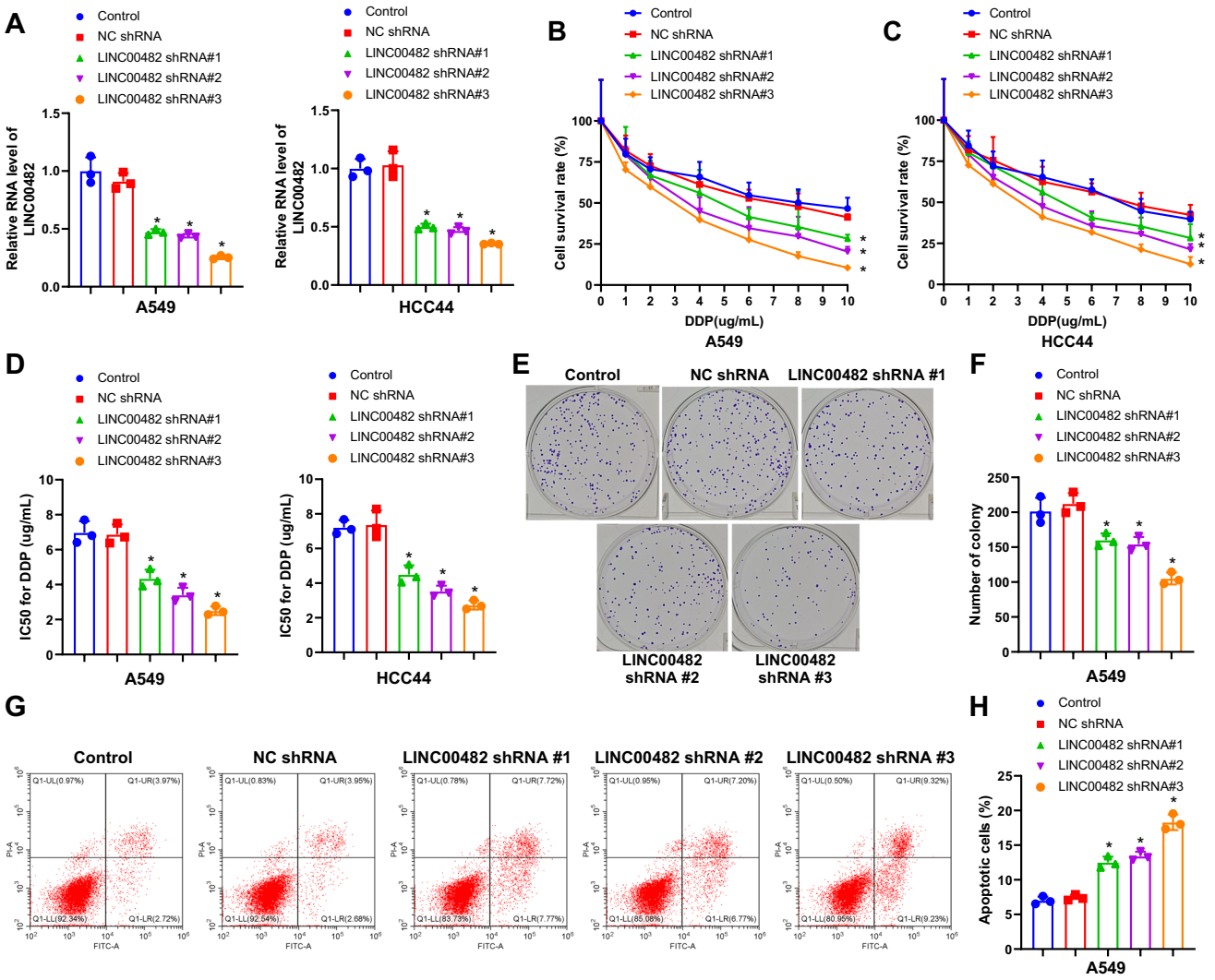


**Fig. 2** Silencing of LINC00482 enhances the sensitivity of NSCLC cells to DDP. Note: A549 and HCC44 cells were infected with LINC00482 shRNAs and treated with different concentrations of DDP. **A**: RT-qPCR to examine the infection efficiency of LINC00482 shRNAs in in A549 and HCC44 cells. B-C: CCK-8 assays to detect the proliferation of A549 (**B**) and HCC44 (**C**) cells after 48 h of stimulation with DDP. **D**: Half inhibition concentration (IC50) of DDP in A549 and HCC44 cells. **E**–**F**: Clone formation assay to assess the clonogenicity of A549 cells. **G**-**H**: Flow cytometry to evaluate apoptosis in A549 cells. The measurement data were displayed as mean ± standard error of mean. Comparisons among multiple groups were performed using one-way analysis of variance with Tukey's multiple comparison tests for post-hoc tests. * indicates $P < 0.05$ compared with the NC shRNA group, $N = 3$. NSCLC, non-small cell lung cancer; DDP, cisplatin

viability of NSCLC cells treated with DDP and also increased the half-inhibitory concentration (IC50) of DDP for A549 and HCC44 cells (Supplementary Fig. 1B-C, $P < 0.05$). Finally, the biological function test of A549 cells showed that oe-LINC00482 transfection enhanced the proliferation and repressed the apoptosis of NSCLC cells (Supplementary Fig. 1D-E, $P < 0.05$).

In summary, LINC00482 knockdown enhanced cell sensitivity to DDP in NSCLC, which could be reversed by LINC00482 overexpression.

## LINC00482 promoted CLASRP expression through recruitment of E2F1

The location of lncRNA in cells is closely associated with its function. Firstly, the location of LINC00482 in A549 cells was examined with RNA-FISH, which manifested that LINC00482 was mainly distributed in the nucleus of A549 cells (Fig. 3A). Further extraction of the different components of A549 cells identified that LINC00482 expression was higher in the nucleus than in the cytoplasm

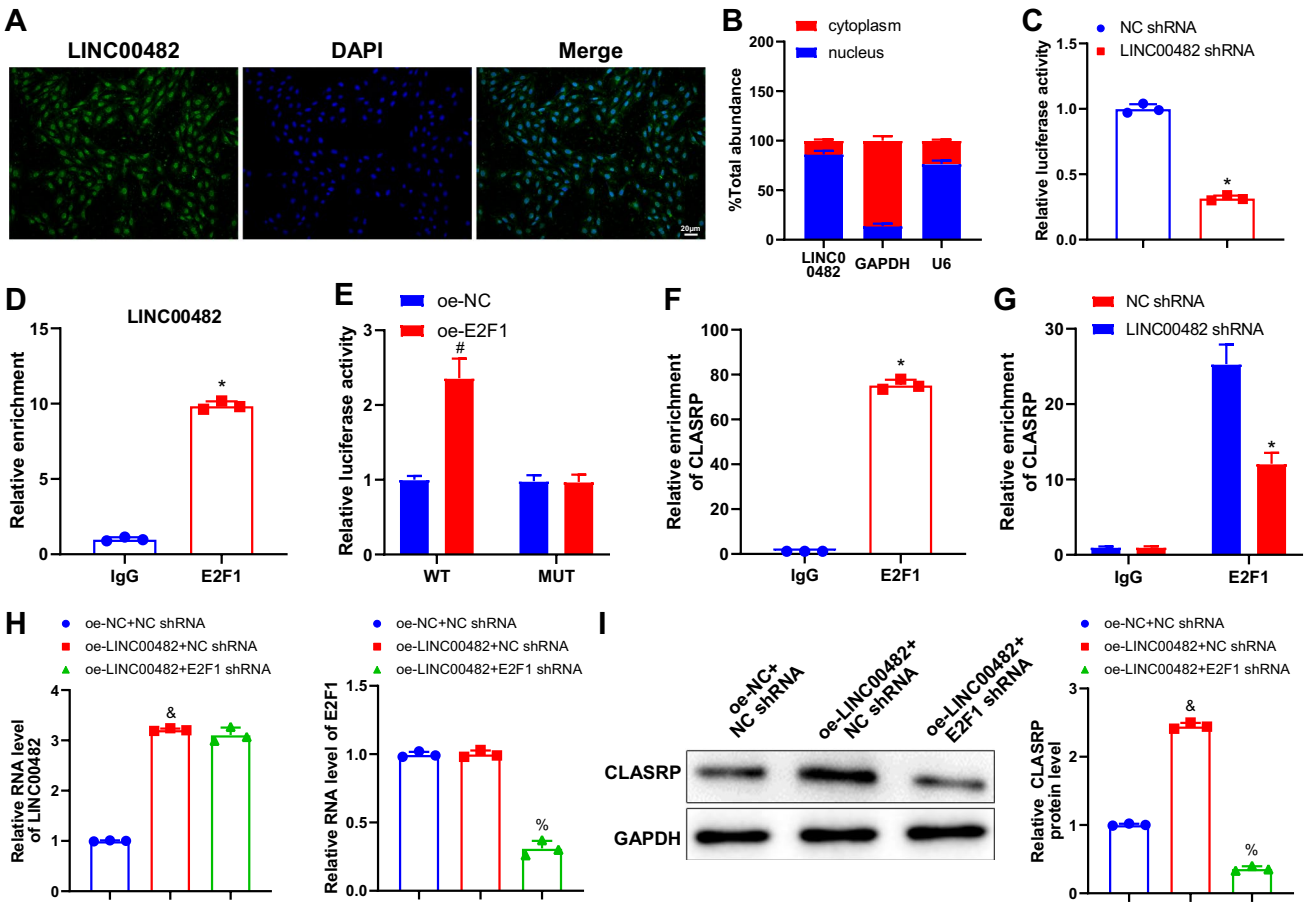


**Fig. 3** LINC00482 recruits E2F1 to promote CLASRP expression. Note: **A**: RNA-FISH to detect LINC00482 location in A549 cells at a scale of 25 μm. **B**: RT-qPCR to assess LINC00482 expression in the cytoplasm and nucleus of A549 cells. **C**: Dual-luciferase reporter assay to analyze the effect of LINC00482 on CLASRP promoter activity in A549 cells after 48-h transfection. **D**: RIP assay to verify the binding of LINC00482 to E2F1. **E**: Dual-luciferase reporter assay to analyze the effect of E2F1 on CLASRP promoter activity in A549 cells after 48-h co-transfection. **F**: ChIP assay to examine the binding of E2F1 to CLASRP. **G**: ChIP assay to examine the regulatory effect of LINC00482 on the binding of E2F1 to CLASRP. **H**: RT-qPCR to assess the transfection efficiency. **I**: Western blotting to measure CLASRP protein expression. The measurement data were displayed as mean ± standard error of mean. Comparisons between the two groups were performed using unpaired *t*-test, and comparisons among multiple groups were analyzed using one-way analysis of variance with Tukey's multiple comparison tests for post-hoc tests. * indicates $P < 0.05$ compared with the NC shRNA or IgG group; # indicates $P < 0.05$ compared with the oe-NC group; & indicates $P < 0.05$ compared with the oe-NC + NC shRNA group; % indicates $P < 0.05$ compared with the oe-LINC00482 + NC shRNA group, $N = 3$

(Fig. 3B, $P < 0.05$), suggesting that it may function mainly by affecting gene transcription. Next, through the LncMAP website, LINC00482 was predicted to participate in NSCLC development by altering CLASRP expression via E2F1. The dual-luciferase reporter assay presented that LINC00482 shRNA notably reduced the CLASRP promoter activity (Fig. 3C. $P < 0.05$), indicating that LINC00482 positively regulated CLASRP expression in A549 cells.

Next, the mechanism that LINC00482 positively regulated CLASRP expression by E2F1 was further tested. RIP assay data confirmed that E2F1 bound more LINC00482 than IgG (Fig. 3D, $P < 0.05$), indicating that E2F1 protein specifically bound LINC00482. The most likely binding sites of E2F1 protein to CLASRP DNA were analyzed with the JASPAR website (Table 3). The dual-luciferase reporter assay demonstrated that oe-E2F1 transfection enhanced the luciferase activity of CLASRP and did not influence the luciferase

**Table 3** Binding sites of E2F1 to CLASRP promoter by JASPAR website

| Matrix ID | Name | Score | Relative score | Sequence ID | Start | End | Strand | Predicted sequence |
|---|---|---|---|---|---|---|---|---|
| MA0024.1 | E2F1 | 7.176547 | 0.813289 | Clasrp | 1736 | 1743 | - | tttgcctc |

activity of CLASRP when the binding sites were mutated (Fig. 3E, P < 0.05), suggesting that the mutated sites were the specific sites where E2F1 protein bound to CLASRP DNA. ChIP assay results manifested that the amplification products obtained with the primers of CLASRP DNA binding sites were signally higher in the E2F1 group than in the IgG group (Fig. 3F, P < 0.05), indicating that the sites of CLASRP DNA (ttttgcctc) were indeed the sites binding to E2F1. The ChIP assay after LINC00482 silencing in A549 cells manifested that LINC00482 silencing apparently reduced E2F1 enrichment in the CLASRP promoter (Fig. 3G, P < 0.05), indicating that only in the presence of LINC00482, E2F1 could bind to the CLASRP promoter to upregulate CLASRP. Subsequently, A549 cells were transfected with oe-LINC00482 and/or E2F1 shRNA. RT-qPCR data revealed excellent transfection efficiencies (Fig. 3H, P < 0.05). Western blotting demonstrated that oe-LINC00482 treatment considerably upregulated CLASRP expression, while further E2F1 shRNA treatment evidently diminished CLASRP expression in the presence of oe-LINC00482 (Fig. 3I, P < 0.05). Summarily, LINC00482 recruited and bound to E2F1 to enhance CLASRP expression in NSCLC cells.

## LINC00482 mediated CLASRP expression in A549 and HCC44 cells

Firstly, The Cancer Genome Atlas (TCGA) database predicted the expression of CLASRP in LUAD, which revealed the upregulation of SFRS16 (CLASRP) in LUAD (Fig. 4A). Meanwhile, to confirm that CLASRP was regulated by LINC00482, LINC00482 was silenced in A549 and HCC44 cells. Results from RT-qPCR and western blotting exhibited that silenced LINC00482 dramatically diminished CLASRP levels in cells (Fig. 4B-D, P < 0.05).

## LINC00482 silencing downregulated CLASRP expression to sensitize NSCLC cells to DDP

To probe the influence of the LINC00482/E2F1/CLASRP axis on NSCLC cell sensitivity to DDP, A549 cells were transfected with LINC00482 shRNA and oe-CLASRP and stimulated with DDP. CCK-8 assay results manifested that oe-CLASRP transfection abrogated LINC00482 shRNA-induced reductions in A549 cell viability after different concentrations of DDP treatment (Fig. 5A, P < 0.05). Subsequently, data from western blotting displayed that LINC00482 shRNA treatment markedly decreased CLASRP expression in DDP-stimulated A549 cells, which was nullified by further oe-CLASRP treatment (Fig. 5B-C, P < 0.05). Clone formation assay and flow cytometry demonstrated that oe-CLASRP nullified the diminishment of clonogenicity and the enhancement of apoptosis in DDP-stimulated A549 cells caused by LINC00482 shRNA (Fig. 5D-G, P < 0.05). Conclusively, LINC00482 knockdown fostered cell sensitivity to DDP in NSCLC by downregulating CLASRP.

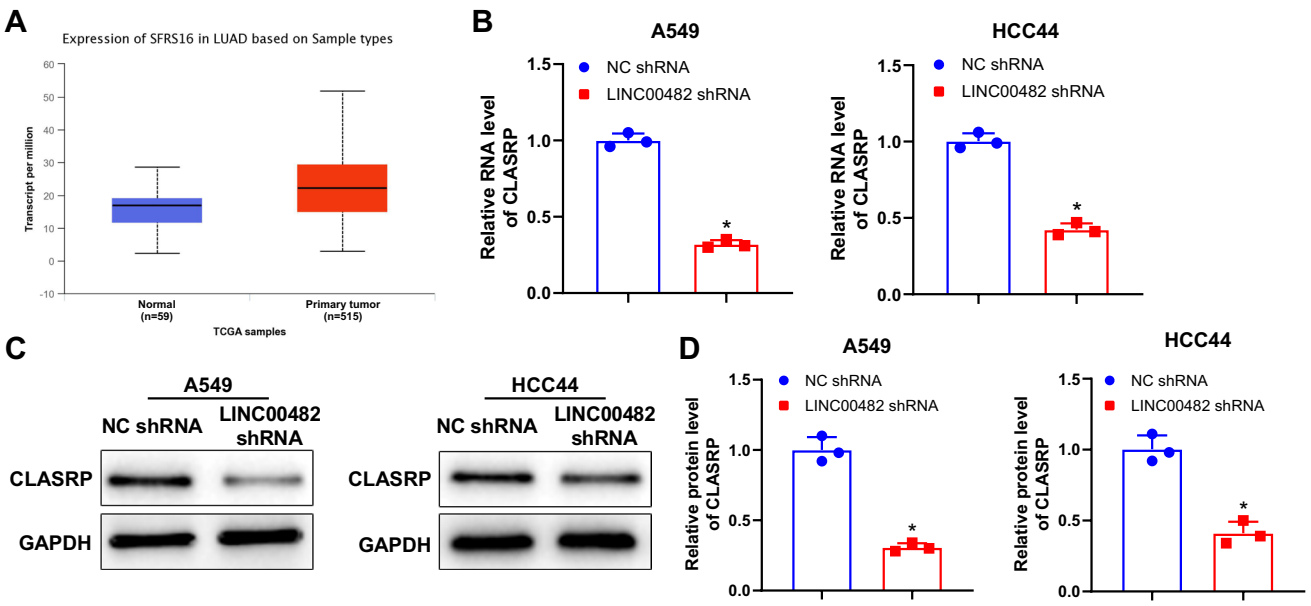


**Fig. 4** LINC00482 promotes CLASRP expression. Note: **A**: Analysis of CLASRP expression in normal and lung cancer samples from TCGA database. **B**: RT-qPCR detection of CLASRP mRNA levels in A549 and HCC44 cells after infection of LINC00482 shRNA. C-D: Protein band plots (**C**) and statistical plots (**D**) of CLASRP protein in A549 and HCC44 cells after infection of LINC00482 shRNA by western blotting. The measurement data were displayed as mean ± standard error of mean. Comparisons between the two groups were performed using unpaired *t*-test. * indicates $P < 0.05$ compared with the NC shRNA group, $N = 3$

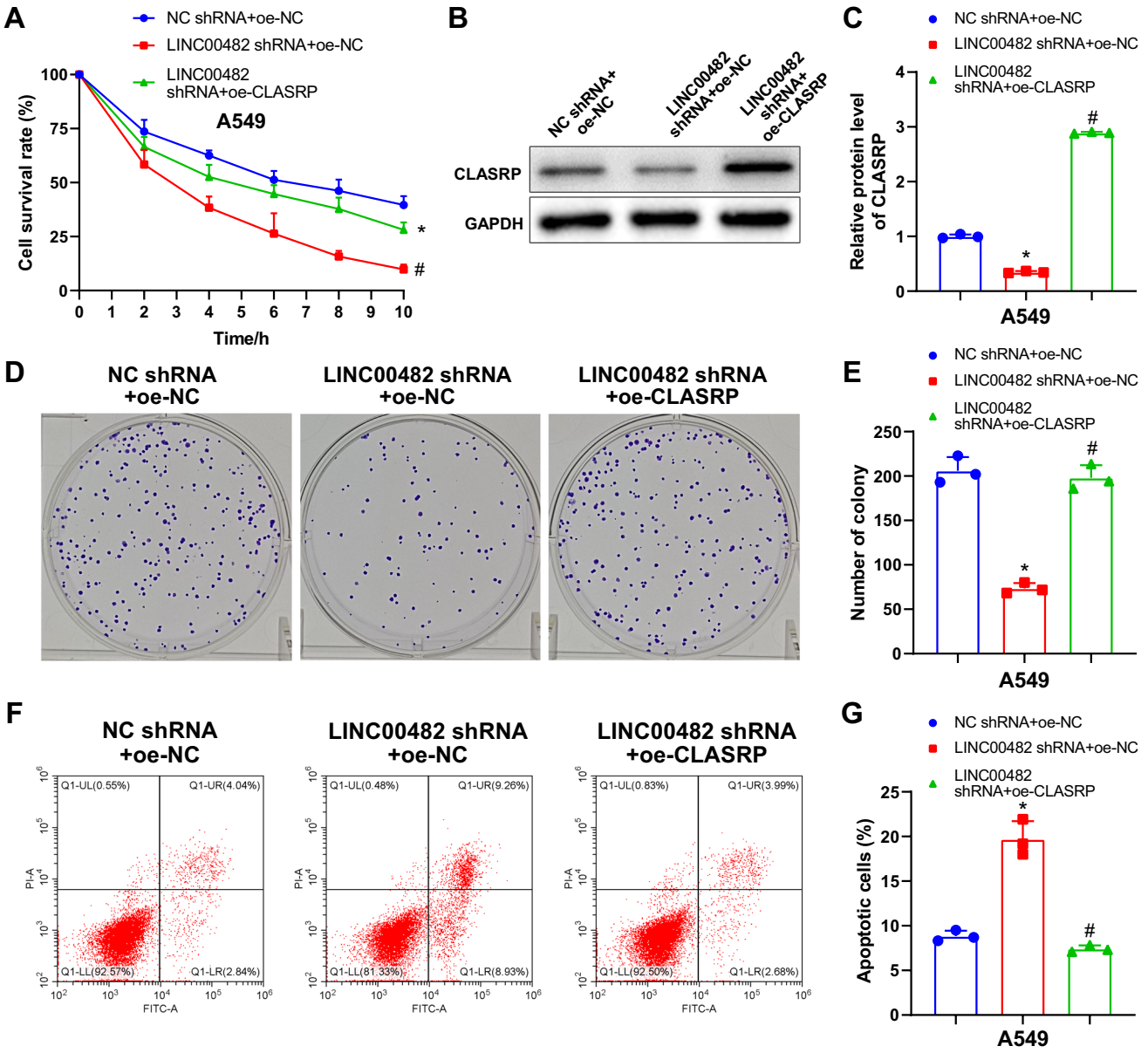


**Fig. 5** Silencing of LINC00482 promotes the sensitivity of NSCLC cells to DDP by downregulating CLASRP. Note: A549 cells were transfected with LINC00482 shRNA and oe-CLASRP and stimulated with DDP. **A**: CCK-8 assay to detect the viability of A549 cells upon stimulation with different concentrations of DDP. After transfection and 48-h stimulation with 6.87 μg/mL (IC50) DDP, **B**-**C**: western blotting to examine CLASRP protein expression in A549 cells; **D**-**E**: clone formation assay to assess the clone formation ability of A549 cells; **F**-**G**: flow cytometry assay to evaluate apoptosis in A549 cells. The measurement data were displayed as mean ± standard error of mean. Comparisons among multiple groups were performed using one-way analysis of variance with Tukey's multiple comparison tests for post-hoc tests. * indicates $P < 0.05$ compared with the NC shRNA + oe-NC group; # indicates $P < 0.05$ compared with the LINC00482 shRNA + oe-NC group, $N = 3$. NSCLC, non-small cell lung cancer; DDP, cisplatin

## LINC00482 silencing restricted tumorigenesis and facilitated sensitivity to DDP in NSCLC in vivo

Nude mice were injected with stably transfected A549 cells and DDP, followed by observation of tumor growth and acquisition of tumor tissues. Results exhibited that both DDP and LINC00482 shRNA remarkably reduced tumor size, volume, and weight in mice (Fig. 6A-C, $P < 0.05$). RT-qPCR and western blotting manifested that both DDP and LINC00482 shRNA conspicuously reduced LINC00482 and CLASRP expression in mouse tumor tissues (Fig. 6D-F, $P < 0.05$). Immunohistochemical staining illustrated that both DDP and LINC00482 shRNA significantly diminished Ki67 positive rate in mouse tumor tissues (Fig. 6G-H,

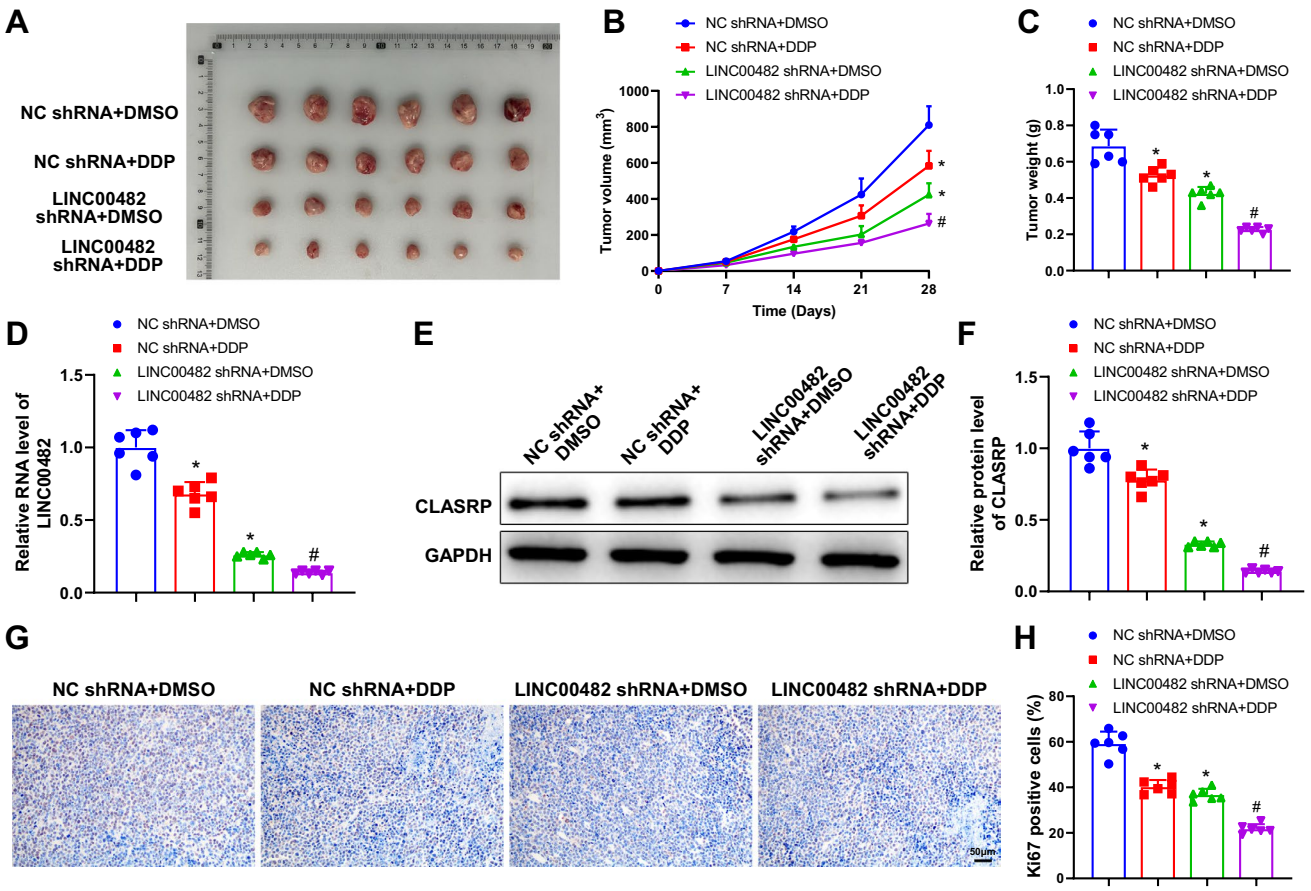


**Fig. 6** Silencing of LINC00482 inhibits tumor growth and enhances the sensitivity to DDP in nude mice. Note: A-C: Statistical plots of size (**A**), volume (**B**), and weight (C) of tumors in nude mice. D: RT-qPCR for LINC00482 and CLASRP levels in tumor tissues. E–F: Western blotting for protein band plots (**E**) and statistical plots (**F**) of CLASRP protein in tumor tissues. **G**-**H**: Immunohistochemical staining for images (**G**) and statistical plots (**H**) of Ki67 positive rate in tumor tissues, scale bar = 50 μm. The measurement data were displayed as mean ± standard error of mean. Comparisons among multiple groups were performed using one-way analysis of variance with Tukey's multiple comparison tests for post-hoc tests. * indicates $P < 0.05$ compared with the NC shRNA + DMSO group; # indicates $P < 0.05$ compared with the NC shRNA + DDP group, $N = 3$. NSCLC, non-small cell lung cancer; DDP, cisplatin

$P < 0.05$). Notably, the combination of LINC00482 shRNA and DDP exerted more substantial effects on the aforementioned genes in mouse tumor tissues than DDP or LINC00482 shRNA alone (Fig. 6A-H, $P < 0.05$). In conclusion, LINC00482 knockdown restrained the growth and enhanced the sensitivity to DDP in NSCLC in vivo.

## Discussion

DDP was approved as an anti-tumor drug in 1978 and today remains a vital and potent treatment for a variety of cancers, including NSCLC and small cell lung cancer (Zhang et al. 2021). Its anticancer effects are related to its capacity to cross-link DNA purine bases, which interferes with DNA repair mechanisms, results in DNA damage, and induces cancer cell apoptosis (Dasari and Tchounwou 2014). However, DDP faces two intrinsic challenges the drug resistance and side effects, which limit its adoption and efficacy (Ghosh 2019). Cancer cells can develop resistance to DDP-induced damage, which generates genetic and epigenetic variations that cause resistance generation and activation of inherent resistance mechanisms of cancer cells (Lugones et al. 2022). Additionally, drug resistance is the leading reason for disease progression and therapeutic failure in NSCLC (Xu et al. 2021). Therefore, investigation of the molecular mechanisms affecting DDP resistance is beneficial to enhancing the efficacy of DDP in NSCLC treatment. This research disclosed that LINC00482 silencing downregulated CLASRP via E2F1 to facilitate the sensitivity to DDP in NSCLC.

Reportedly, some lncRNAs participate in DDP resistance in NSCLC via influence on signaling pathways, modulation of repair factors, and regulation of nearby genes, suggesting that targeting lncRNAs is a promising strategy to reverse chemotherapy resistance to DDP in NSCLC (Wang et al. 2018). For instance, lncRNA small nucleolar RNA host gene

1 facilitates DDP resistance, metastasis, and proliferation of NSCLC cells through the miR-330-5p/doublecortin-like kinase protein 1 axis (Ge et al. 2021). LncRNA Forkhead box D3 antisense RNA1 upregulates mouse double minute 2 level by decreasing miR-127-3p to enhance DDP resistance in NSCLC (Zeng et al. 2020). Knockdown of lncRNA TatD DNase domain containing 1 diminishes tripartite motif 66 level to enhance DDP sensitivity in NSCLC by augmenting miR-451 (Wang et al. 2019). Of note, LINC00482 acts as an oncogene in various cancers. For instance, LINC00482/hsa-miR-6756-3p/regulator of calcineurin 2 may exert vital functions in the progression of chronic pancreatitis to pancreatic ductal adenocarcinoma (Zhao et al. 2023). LINC00482 is related to the overall survival of patients with alpha-fetoprotein-negative hepatocellular carcinoma (Liu et al. 2021). LINC00482 is upregulated in bladder cancer tissues and cells and facilitates angiogenesis and inflammation in bladder cancer through upregulation of the forkhead box A1/matrix metalloproteinase15 axis (Wang et al. 2020). Moreover, Zhang et al. uncovered that LINC00482 expression was upregulated in LUSC cell lines and tissues (Zhang et al. 2022a, b). Concordantly, this research identified high LINC00482 expression in NSCLC tissues and cells. However, the influence of LINC00482 on DDP resistance in NSCLC has not been discovered. Interestingly, this research unveiled that LINC00482 knockdown reduced viability and clone formation and elevated apoptosis in DDP-stimulated NSCLC cells, thereby enhancing cell sensitivity to DDP in NSCLC. Further data from gain-of-function assays revealed that upregulated LINC00482 restrained NSCLC cell sensitivity to DDP. Tumor-bearing mouse assays validated that LINC00482 knockdown restrained tumor growth and enhanced DDP sensitivity in mice.

Next, the mechanism of LINC00482 on DDP resistance in NSCLC was predicted by website and bioinformatics analyses, indicating that the actions of LINC00482 in NSCLC may be achieved by modulating E2F1 to affect CLASRP levels. Through a series of experiments, we observed that LINC00482 was mainly localized in the cell nucleus and that LINC00482 recruited E2F1 to enhance CLASRP expression in NSCLC cells. As a member of the E2F family, which is associated with cell cycle, E2F1 is primarily engaged in a variety of cellular processes, like DNA repair, proliferation, cell differentiation, cell cycle progression, apoptosis, and DNA replication (Zou et al. 2020). Considerable evidence demonstrates that E2F1 as an oncogene can contribute to malignant behaviors in NSCLC cells (Li et al. 2021; Lv et al. 2021; Wang and Wang 2020). Of note, E2F1 may enhance DDP sensitivity in NSCLC cells via upregulation of solute carrier family 7 member 2 expression (Jiang et al. 2023). miR-26a depressed DDP resistance in human NSCLC by down-regulating the High mobility group A-mediated E2F1-protein kinase B pathway (Yang et al. 2016). These studies indicate that E2F1 is implicated in the sensitivity to DDP in NSCLC. A prior study unraveled that CLASRP was related to poor prognosis in patients with clear cell renal carcinoma (Yang et al. 2021). CLASRP exerts essential functions in cancer progression and is an independent prognostic factor for patients with head and neck cancer (Liang et al. 2019). However, no studies have explored the association between CLASRP and NSCLC. Our data identified that CLASRP expression was upregulated in LUAD and LUSC samples and that CLASRP overexpression counterweighed the facilitation of LINC00482 knockdown on DDP sensitivity in NSCLC.

## Conclusions

In conclusion, this research first uncovered the roles of LINC00482 and CLASRP in NSCLC. LINC00482 knockdown facilitate the sensitivity to DDP in NSCLC by inactivating the E2F1/CLASRP axis. This research presents a novel view that treatment targeting LINC00482 knockdown may enhance the efficacy of DDP, which is beneficial for NSCLC management. However, a limitation of this research is that no further clinical trials were conducted. Therefore, the future challenge will be devoted to the research in clinical trials, which may provide novel targets for the clinical treatment and management of NSCLC.

**Supplementary Information** The online version contains supplementary material available at https://doi.org/10.1007/s10142-023-01260-4

**Author contribution** LYM conceived the ideas. LYM, LJM and LSJ designed the experiments. LYM, LJM, LSJ, CYT and LYP performed the experiments. LYM, LJM and LSJ analyzed the data. LYM, YZX and WYC provided critical materials. LYM, CYT and LYP wrote the manuscript. YZX and WYC supervised the study. All the authors have read and approved the final version for publication.

**Funding** Thanks for the grant from the Affiliated Hospital of Guangdong Medical University Clinical Research Project in Hospital Fund (No. LCYJ2021B005).

**Data availability** The datasets used or analyzed during the current study are available from the corresponding author on reasonable request.

## Declarations

**Competing interests** The authors declare that they have no competing interests.

## References

Ayuk SM, Abrahamse H, Houreld NN (2016) The role of photobiomodulation on gene expression of cell adhesion molecules in diabetic wounded fibroblasts in vitro. J Photochem Photobiol B 161:368–374. https://doi.org/10.1016/j.jphotobiol.2016.05.027

Dasari S, Tchounwou PB (2014) Cisplatin in cancer therapy: molecular mechanisms of action. Eur J Pharmacol 740:364–378. https://doi.org/10.1016/j.ejphar.2014.07.025

Dohopolski M, Gottumukkala S, Gomez D, Iyengar P (2021) Radiation therapy in non-small-cell lung cancer. Cold Spring Harb Perspect Med 11. https://doi.org/10.1101/cshperspect.a037713

Fan XX, Wu Q (2022) Decoding lung cancer at single-cell level. Front Immunol 13:883758. https://doi.org/10.3389/fimmu.2022.883758

Fouad S, Hauton D, D'Angiolella V (2020) E2F1: cause and consequence of dna replication stress. Front Mol Biosci 7:599332. https://doi.org/10.3389/fmolb.2020.599332

Ge P, Cao L, Zheng M, Yao Y, Wang W, Chen X (2021) LncRNA SNHG1 contributes to the cisplatin resistance and progression of NSCLC via miR-330-5p/DCLK1 axis. Exp Mol Pathol 120:104633. https://doi.org/10.1016/j.yexmp.2021.104633

Ghosh S (2019) Cisplatin: the first metal based anticancer drug. Bioorg Chem 88:102925. https://doi.org/10.1016/j.bioorg.2019.102925

Jiang S, Zou J, Dong J, Shi H, Chen J, Li Y, Duan X, Li W (2023) Lower SLC7A2 expression is associated with enhanced multidrug resistance, less immune infiltrates and worse prognosis of NSCLC. Cell Commun Signal 21:9. https://doi.org/10.1186/s12964-022-01023-x

Kryczka J, Kryczka J, Czarnecka-Chrebelska KH, Brzezianska-Lasota E (2021) Molecular mechanisms of chemoresistance induced by cisplatin in NSCLC cancer therapy. Int J Mol Sci 22. https://doi.org/10.3390/ijms22168885

Kun-Peng Z, Xiao-Long M, Chun-Lin Z (2017) LncRNA FENDRR sensitizes doxorubicin-resistance of osteosarcoma cells through down-regulating ABCB1 and ABCC1. Oncotarget 8:71881–71893. https://doi.org/10.18632/oncotarget.17985

Li H, Chen YK, Wan Q, Shi AQ, Wang M, He P, Tang LX (2021) Long Non-coding RNA LINC00847 Induced by E2F1 accelerates non-small cell lung cancer progression through targeting miR-147a/IFITM1 Axis. Front Med (lausanne) 8:663558. https://doi.org/10.3389/fmed.2021.663558

Liang Y, Song J, He D, Xia Y, Wu Y, Yin X, Liu J (2019) Systematic analysis of survival-associated alternative splicing signatures uncovers prognostic predictors for head and neck cancer. J Cell Physiol 234:15836–15846. https://doi.org/10.1002/jcp.28241

Lin X, Han T, Xia Q, Cui J, Zhuo M, Liang Y, Su W, Wang L, Wang L, Liu Z, Xiao X (2021) CHPF promotes gastric cancer tumorigenesis through the activation of E2F1. Cell Death Dis 12:876. https://doi.org/10.1038/s41419-021-04148-y

Liu Z, Pu Y, Bao Y, He S (2021) Investigation of potential molecular biomarkers for diagnosis and prognosis of AFP-negative HCC. Int J Gen Med 14:4369–4380. https://doi.org/10.2147/IJGM.S323868

Lu G, Li Y, Ma Y, Lu J, Chen Y, Jiang Q, Qin Q, Zhao L, Huang Q, Luo Z, Huang S, Wei Z (2018) Long noncoding RNA LINC00511 contributes to breast cancer tumourigenesis and stemness by inducing the miR-185-3p/E2F1/Nanog axis. J Exp Clin Cancer Res 37:289. https://doi.org/10.1186/s13046-018-0945-6

Lugones Y, Loren P, Salazar LA (2022) Cisplatin resistance: genetic and epigenetic factors involved. Biomolecules 12. https://doi.org/10.3390/biom12101365

Lv X, Lian Y, Liu Z, Xiao J, Zhang D, Yin X (2021) Exosomal long non-coding RNA LINC00662 promotes non-small cell lung cancer progression by miR-320d/E2F1 axis. Aging (Albany NY) 13:6010–6024. https://doi.org/10.18632/aging.202522

Miller M, Hanna N (2021) Advances in systemic therapy for non-small cell lung cancer. BMJ 375:n2363. https://doi.org/10.1136/bmj.n2363

Shan KZ, Yang SF, Deng YJ, Yue PY, Du ZQ (2022) E2F1-induced long non-coding RNA MCF2L-AS1 modulates Cyclin D1 mRNA stability through ELAVL1 to induce Gefitinib resistance in non-small cell lung cancer. Acta Biochim Pol 69:795–804. https://doi.org/10.18388/abp.2020_6118

Sun R, Wang R, Chang S, Li K, Sun R, Wang M, Li Z (2019) Long non-coding RNA in drug resistance of non-small cell lung cancer: a mini review. Front Pharmacol 10:1457. https://doi.org/10.3389/fphar.2019.01457

Suster DI, Mino-Kenudson M (2020) Molecular pathology of primary non-small cell lung cancer. Arch Med Res 51:784–798. https://doi.org/10.1016/j.arcmed.2020.08.004

Tan D, Li G, Zhang P, Peng C, He B (2022) LncRNA SNHG12 in extracellular vesicles derived from carcinoma-associated fibroblasts promotes cisplatin resistance in non-small cell lung cancer cells. Bioengineered 13:1838–1857. https://doi.org/10.1080/21655979.2021.2018099

Wang A, Wang J (2020) E2F1-induced overexpression of long non-coding RNA SBF2-AS1 promotes non-small-cell lung cancer metastasis through regulating miR-362-3p/GRB2 Axis. DNA Cell Biol 39:1290–1298. https://doi.org/10.1089/dna.2020.5426

Wang L, Ma L, Xu F, Zhai W, Dong S, Yin L, Liu J, Yu Z (2018) Role of long non-coding RNA in drug resistance in non-small cell lung cancer. Thorac Cancer 9:761–768. https://doi.org/10.1111/1759-7714.12652

Wang L, Shang X, Feng Q (2019) LncRNA TATDN1 contributes to the cisplatin resistance of non-small cell lung cancer through TATDN1/miR-451/TRIM66 axis. Cancer Biol Ther 20:261–271. https://doi.org/10.1080/15384047.2018.1529091

Wang Y, Zhang L, Wei N, Sun Y, Pan W, Chen Y (2020) Silencing LINC00482 inhibits tumor-associated inflammation and angiogenesis through down-regulation of MMP-15 via FOXA1 in bladder cancer. Aging (Albany NY) 13:2264–2278. https://doi.org/10.18632/aging.202247

Wang X, Chen Y, Dong K, Ma Y, Jin Q, Yin S, Zhu X, Wang S (2021) Effects of FER1L4-miR-106a-5p/miR-372-5p-E2F1 regulatory axis on drug resistance in liver cancer chemotherapy. Mol Ther Nucleic Acids 24:449–461. https://doi.org/10.1016/j.omtn.2021.02.006

Wang W, Wang J, Liu S, Ren Y, Wang J, Liu S, Cui W, Jia L, Tang X, Yang J, Wu C, Wang L (2022) An EHMT2/NFYA-ALDH2 signaling axis modulates the RAF pathway to regulate paclitaxel resistance in lung cancer. Mol Cancer 21:106. https://doi.org/10.1186/s12943-022-01579-9

Xie H, Yao J, Wang Y, Ni B (2022) Exosome-transmitted circVMP1 facilitates the progression and cisplatin resistance of non-small cell lung cancer by targeting miR-524-5p-METTL3/SOX2 axis. Drug Deliv 29:1257–1271. https://doi.org/10.1080/10717544.2022.2057617

Xu Z, Lie RT, Wilcox AJ, Saugstad OD, Taylor JA (2019) A comparison of DNA methylation in newborn blood samples from infants with and without orofacial clefts. Clin Epigenetics 11:40. https://doi.org/10.1186/s13148-019-0638-9

Xu R, Luo X, Ye X, Li H, Liu H, Du Q, Zhai Q (2021) SIRT1/PGC-1alpha/PPAR-gamma correlate with hypoxia-induced chemoresistance in non-small cell lung cancer. Front Oncol 11:682762. https://doi.org/10.3389/fonc.2021.682762

Yang Y, Zhang P, Zhao Y, Yang J, Jiang G, Fan J (2016) Decreased MicroRNA-26a expression causes cisplatin resistance in human non-small cell lung cancer. Cancer Biol Ther 17:515–525. https://doi.org/10.1080/15384047.2015.1095405

Yang F, Zhao J, Luo X, Li T, Wang Z, Wei Q, Lu H, Meng Y, Cai K, Lu L, Lu Y, Chen L, Sooranna SR, Luo L, Song J, Meng L (2021) Transcriptome profiling reveals B-lineage cells contribute to the poor prognosis and metastasis of clear cell renal cell carcinoma. Front Oncol 11:731896. https://doi.org/10.3389/fonc.2021.731896

Zeng Z, Zhao G, Zhu H, Nie L, He L, Liu J, Li R, Xiao S, Hua G (2020) LncRNA FOXD3-AS1 promoted chemo-resistance of NSCLC cells via directly acting on miR-127-3p/MDM2 axis. Cancer Cell Int 20:350. https://doi.org/10.1186/s12935-020-01402-9

Zhang XD, Huang GW, Xie YH, He JZ, Guo JC, Xu XE, Liao LD, Xie YM, Song YM, Li EM, Xu LY (2018) The interaction of lncRNA EZR-AS1 with SMYD3 maintains overexpression of EZR in ESCC cells. Nucleic Acids Res 46:1793–1809. https://doi.org/10.1093/nar/gkx1259

Zhang J, Ye ZW, Tew KD, Townsend DM (2021) Cisplatin chemotherapy and renal function. Adv Cancer Res 152:305–327. https://doi.org/10.1016/bs.acr.2021.03.008

Zhang L, Zhang Y, Wang C, Yang Y, Ni Y, Wang Z, Song T, Yao M, Liu Z, Chao N, Yang Y, Shao J, Li Z, Zhou R, Chen L, Zhang D, Zhao Y, Liu W, Li Y, He P, Lin JW, Wang Y, Zhang K, Chen L, Li W (2022a) Integrated single-cell RNA sequencing analysis reveals distinct cellular and transcriptional modules associated with survival in lung cancer. Signal Transduct Target Ther 7:9. https://doi.org/10.1038/s41392-021-00824-9

Zhang Y, Wang Y, Yin X, Huang Y (2022b) Identification of pyroptosis-related long non-coding RNAs with prognosis and therapy in lung squamous cell carcinoma. Sci Rep 12:11206. https://doi.org/10.1038/s41598-022-15373-6

Zhao Z, Luo Q, Liu Y, Jiang K, Zhou L, Dai R, Wang H (2023) Multilevel integrative analysis of the roles of lncRNAs and differential mRNAs in the progression of chronic pancreatitis to pancreatic ductal adenocarcinoma. BMC Genomics 24:101. https://doi.org/10.1186/s12864-023-09209-4

Zou L, Lei H, Shen J, Liu X, Zhang X, Wu L, Hao J, Jiang W, Hu Z (2020) HO-1 induced autophagy protects against IL-1 beta-mediated apoptosis in human nucleus pulposus cells by inhibiting NF-kappaB. Aging (Albany NY) 12:2440–2452. https://doi.org/10.18632/aging.102753